



Research Article

The effect of different sliding speeds on wear behavior of ZrO₂ reinforcement aluminium matrix composite materials

İjlal Şimşek ^{a,*} , Doğan Şimşek ^b  and Dursun Özyürek ^c 

^aKarabuk University, TOBB Technical Sciences Vocational School, Karabuk, 78050, Turkey

^bNational Defense University, Land Forces NCO Vocational School, Balıkesir, 10100, Turkey

^cKarabuk University, Technology Faculty, Karabuk, 78050, Turkey

ARTICLE INFO

Article history:

Received 17 January 2020

Revised 24 March 2020

Accepted 29 March 2020

Keywords:

Al composite

Mechanical alloying

Wear

ZrO₂

ABSTRACT

Due to the many advantages it provides metal matrix composite materials, it is used as a publication in many industrial applications, especially in the automotive industry. Therefore, it is necessary to know the properties of these materials such as mechanical, tribological and corrosion. In this study, the effect of different sliding speeds was investigated on wear behavior of aluminum matrix composite materials produced by adding different amounts of ZrO₂ by mechanical alloying method. 4 different amounts (3%, 6%, 9% and 12%) ZrO₂ were added to the aluminum 2% graphite matrix. Composite powders mechanically alloyed for 60 minutes, were produced green compact samples by cold pressed with a pressure of 700 MPa. The green compacts produced were sintered for 2 hours at 600 °C. The produced aluminum composites were characterized by microstructure, density and hardness measurements. Wear tests were carried out on a block on-ring type wear testing device, under 20 N load and three different sliding speed (0.2 ms⁻¹, 0.4 ms⁻¹ and 0.6 ms⁻¹) and three different sliding distances (53 m, 72 m and 94 m). As a result of the studies, hardness and density values increased as the amount of ZrO₂ in the matrix increased. Wear test results showed that weight loss decreased with increasing amount of reinforcement in the matrix.

© 2020, Advanced Researches and Engineering Journal (IAREJ) and the Author(s).

1. Introduction

Aluminium and its alloys are commonly used in aviation, automotive and defence sectors due to their low density, good mechanical properties and good corrosion properties [1,2]. However, relatively low wear resistance of aluminium and its alloys despite good mechanical properties restricts the use of these alloys in some tribological applications. The aluminium matrix composites (AMCs) display better wear performance when compared to aluminium alloys [3-5]. AMCs are manufactured with the continuous addition of fibre, short fibre and particle reinforcements. In many studies related to AMCs, it is reported that carbides [6-8], nitrides [9] and oxides [10, 11] are used as reinforcement agent. Particle reinforced AMCs are commonly used owing to their availability, low costs, mechanical properties and variety of production methods [12-14]. Along with these

advantages, AMCs have other features such as high elasticity module, high hardness, good electricity, thermal conductivity and good corrosion resistance, as well [4, 12]. AMCs can be manufactured through fluid (infiltration) [15], solid (powder metallurgy) [16-20] and semi-solid (thixo-moulding) [21-23] methods. Prabhu et al. [24] reports that powder metallurgy (PM) offers numerous advantages and thus, this technology is more preferred in the production of AMCs. The biggest advantage of the PM method for AMC is that the reinforcement material can properly disperse within the matrix. Powder metallurgy method essentially consists of three phases: mixing the powders, pressing and sintering. Furthermore, mechanical alloying (MA), which is a powder metallurgy method, is preferred in the production of AMCs with better mechanical properties when compared to the other particle reinforced composite production methods [16]. In many studies, it was reported that reinforcement materials such

* Corresponding author. Tel.: +90 370 418 9081; Fax: +90 370 418 9345.

E-mail addresses: ijlalispir@karabuk.edu.tr (I. Şimşek), densimsek@outlook.com (D. Şimşek), dozyurek@karabuk.edu.tr (D. Özyürek)

ORCID: 0000-0001-6542-8567 (I. Şimşek), 0000-0001-8339-9704 (D. Şimşek), 0000-0002-8326-9982 (D. Özyürek)

DOI: 10.35860/iarej.676152

as Al₂O₃ [11, 15, 18] and SiC [6, 16, 23, 25] improved the wear resistance of AMC materials. Zirconia (ZrO₂) is considered as a good reinforcement material in AMC materials owing to its high hardness and high elasticity module. However, it has high thermal stability and thermal shock resistance at high temperatures. [1, 26]. Baghchesara et al. [27] reported in their study that the AMC materials produced at different casting temperatures with the addition of different amounts of ZrO₂ had improved mechanical properties thanks to the increasing amounts of ZrO₂ reinforcements. In their study, Ramachandra et al. [28] stated that weight loss decreased with the increasing amount of ZrO₂ added into the matrix. In the studies conducted in the literature, ZrO₂ reinforcement has been addressed in a limited manner.

In the present study, AMC materials were produced with the addition of different amounts of ZrO₂ into Al-%2 graphite matrix by using the MA method. The study aimed to determine the effects of ZrO₂ added into the AMC materials on microstructure, hardness and wear behaviours at different sliding speeds.

2. Materials and Method

In the experimental studies, aluminum (Al) powder (vol.%) having a size of <50 µm and a purity of 99.5% and graphite of 2% having a size of <40 µm were used as the matrix material. The Al matrix was reinforced with ZrO₂ (vol.%) having a powder size of 0-50 µm in three different amounts (3%, 6% 9% and 12%). The chemical composition of the AMCs powders produced is provided in Table 1.

The powders having the chemical composition given in Table 1 are mechanically alloyed in a planetary mill. During mechanical alloying (MA) processes, a stainless steel milling cell (400 ml), stainless steel balls having a diameter of 10 mm, a ball to powder ratio of 1:10, 1% of ethanol is used to prevent agglomeration, and a milling time of 60 minutes were used in the atmospheric environment. Mechanical alloying was performed in 30 minute periods. It was allowed to stand for 10 minutes between the periods to prevent the dust from overheating. In the mechanical alloying process, Fritsch Pulverisette brand planetary type mechanical alloying device was used. After mechanical alloying, powder size analysis was made from 12% ZrO₂ added composite powder. Particle analyzer Malvern brand 3000 was used for powder size analysis.

The average powder size of composite powders with 12% ZrO₂ added, (D50) is 55.89 µm. Mechanically alloyed Al composite powders were cold pressed (700 MPa) and green compacts of Ø10x7 mm were produced. The produced green compacts were sintered at 600 °C under argon for 120 minutes and cooled to room temperature in a furnace.

Table 1. Chemical composition of AMCs powders produced

Sample	Al (wt.%)	Grafit (wt.%)	ZrO ₂ (wt.%)
AlGr	98	2	---
AlGr3ZrO ₂	95	2	3
AlGr6ZrO ₂	92	2	6
AlGr9ZrO ₂	89	2	9
AlGr12ZrO ₂	86	2	12

Standard metallographic treatments were applied for the microstructure analyses and the samples prepared were etched with a solution of 2 ml HF, 3 ml HCl, 20 ml HNO₃, 175 ml H₂O (Keller's) solution for 10-15 seconds. Microstructure analyzes of the etched samples were carried out by Carl Zeiss Ultra Plus Gemini Scanning Electron Microscope and Electron Diffraction Spectroscopy (SEM). In addition, the sintered samples were made by Rigaku brand XRD (X-ray diffraction) device. However, samples were characterized hardness and density measurements. Density measurements were made using density measurement kit in Precisa XB200h brand precision scale according to Archimedes' principle [29]. Density measurements were taken on three samples and averaged. Hardness measurements were taken with using Shimadzu microhardness tester for 10 seconds by using HMV2. The hardness measurements were obtained by using three different samples, at five different points and used averaged. Wear tests were carried out at four different sliding distances (53 m, 72 m and 94 m) at three different sliding speeds (0.2 ms⁻¹, 0.4 ms⁻¹ and 0.6 ms⁻¹) under different loads of 20 N on a pin on disc wear test device according to ASTM G99-05 standard [30]. The sliding distance used in the wear tests was determined according to stopping distances of a vehicle in different speeds [31]. Before each wear test, the surface of samples and disks were cleaned with acetone. In the wear tests, three different samples were tested for each parameter and the results were averaged. Wear rates were calculated by the equation given in Equation 1 using the weight loss results obtained [30].

$$W_a = \Delta m / (M \cdot s \cdot \rho) \quad (1)$$

Wherein, W_a is the wear rate, Δm is the weight loss (g) obtained after the wear test, M is the load (N) used in the tests, s is the sliding distance (m), and ρ is the density (g/cm³) of the wear sample. After the wear test, worn surface SEM images were examined and the active wear mechanisms were tried to be determined.

3. Results and Discussion

3.1 Microstructure examinations

Microstructure SEM images of composite materials produced by adding different amounts of ZrO₂ are given in Figure 1.

When the SEM images of AMC materials produced with the addition of different amounts of ZrO₂ given in Figure 1 are examined, insoluble graphite particles (grey areas 2. location) are observed in the matrix material (Figure 1.a). It is seen that these graphite particles in the matrix material are not coarse particles as the amount of reinforcement material increases. The reason why graphite particles are observed in the structure is that it further contracted with the influence of hard reinforcement particles added into the matrix along with high-energy balls during MA. Table 2 shows the EDS analysis results of AMC materials with different amounts of ZrO₂ added.

In the study conducted by Şimşek [32], similar results were obtained. Furthermore, Chu et al. [33] reported that smaller graphite particles fully turned into Al₄C₃ compound and bigger ones appeared as graphite particles. Also, the SEM images show that ZrO₂ added into the matrix (light grey areas, 4. location) are particularly located on the grain boundaries. Sekar et al. [34] and Baghchesara et al. [27] stated in their studies that ZrO₂ tended to agglomerate on the grain boundaries. XRD analysis results of composite materials after the addition of AlGr and 12% ZrO₂ are given in Figure 2.

When the XRD results of AMC materials after the addition of AlGr and 12% ZrO₂ are examined, it is seen that the matrix material (AlGr) has Al (Card number: 9011602) and graphite (Card number: 00-056-0159). However, Al₄C₃ (Card number: 00-035-0799) phase, which was expected to occur in the matrix, cannot be observed. The failure to observe Al₄C₃ in the structure is attributed to the low range of XRD scan or nanosize of Al₄C₃ forming in the structure.

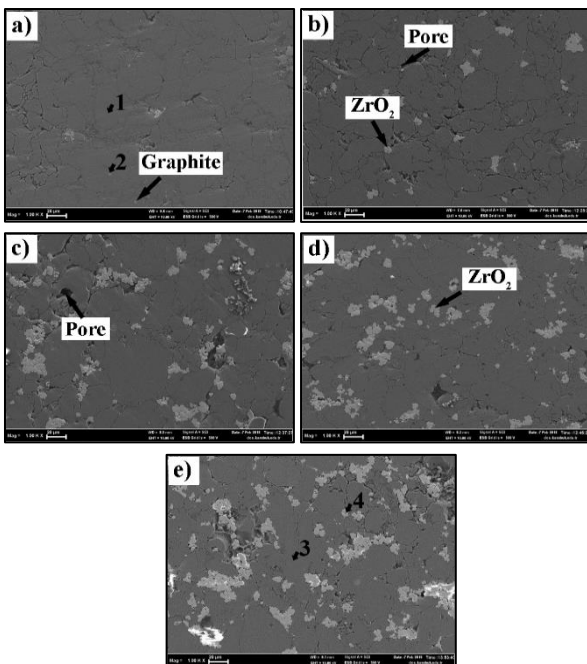


Figure 1. Microstructural SEM images of composite materials with different amounts of ZrO₂ reinforcement; AlGr (a), 3% ZrO₂ (b), 6% ZrO₂ (c), 9% ZrO₂ (d) and 12% ZrO₂ (e).

Table 2. EDS analysis results of AMC materials with different amounts of ZrO₂

Location	Al	C	Zr	O
1	93.22	4.64	-	2.14
2	81.23	12.15	-	6.62
3	94.14	3.73	-	1.45
4	0.71	3.73	66.59	28.97

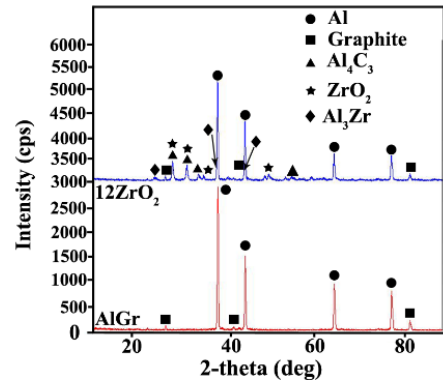


Figure 2. XRD result of the composite material produced with AlGr and 12% ZrO₂ reinforcement.

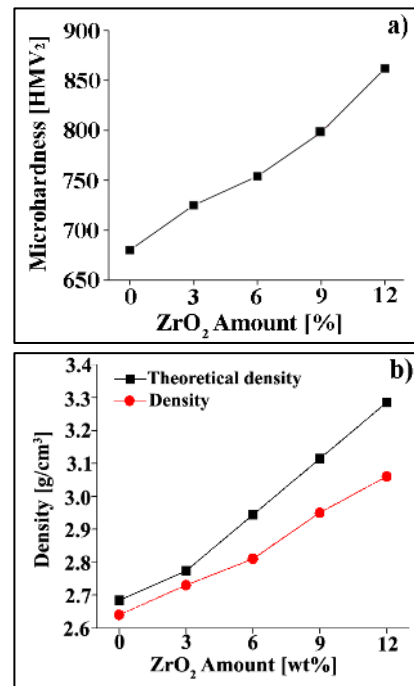


Figure 3. Changes in hardness (a) and density (b) of composite materials with different amounts of ZrO₂ reinforcement

In their study, Bostan et al. [35] reported that Al₄C₃ compounds formed at nano size in Al-C system produced with MA method. However, in the XRD results of the AMC material with 12% ZrO₂ added, it was observed that Al₃Zr (Card number: 01-074-5295) phase formed along with the expected Al₄C₃ phase. The presence of Al₄C₃ phase in the structure of AMC material after the addition of 12% ZrO₂ is due to the fact that graphite further contracts and fully dissolves in the structure with the influence of hard reinforcement particles during MA. Hardness and density results of AMC materials after the

addition of different amounts of ZrO_2 are given in Figure 3.

When the hardness results of the AMC materials after the addition of different amounts of ZrO_2 as given in Figure 3.a are examined, it is seen that hardness increases as the amount of reinforcement increase. While the lowest hardness value was obtained as 680 HMV in matrix material (AlGr), the highest hardness value was obtained as 862 HMV in the AMC material with the addition of 12% ZrO_2 . The increase in hardness is attributed to the hard secondary phase particles ex-situ added into the matrix and the dislocation accumulation occurring on the matrix interface. Das et al. [1] obtained similar results in ZrO_2 reinforced composite materials produced with the casting method. They reported that the hardness increased since a dislocation accumulation occurred on the matrix-reinforcement interface during cooling due to the lower coefficient of thermal expansion of the reinforcement material (ZrO_2) when compared to Al. Again when the density changes of the AMC materials with the addition of different amounts of ZrO_2 as given in Figure 3.b are examined, it is seen that density increases as the amount of reinforcement increases. While the lowest density value was obtained as 2.6 g/cm^3 in the matrix material, the highest density value was obtained as 3.06 g/cm^3 in the AMC material after the addition of 12% ZrO_2 . Based on the results, it can be stated that the density values increased as expected. This increase in the density values results from higher density of the reinforcement material (ZrO_2 5.68 g/cm^3) than the matrix material (AlGr 2.64 g/cm^3). Similar results were obtained in the previously conducted studies [27, 36]. Data related to the weight losses and wear rates of the AMC materials after the addition of different amounts of ZrO_2 are given in Figure 4.

When the weight losses of the AMC materials containing different amounts of ZrO_2 at different sliding speeds as given in Figure 4 are examined, it is seen that, as expected, weight loss decreases at all sliding speeds as the amount of ZrO_2 increases. The obtained results are compatible with the hardness results given in Figure 3. However, a sudden increase is observed in the weight loss results of the AMC material containing 6% ZrO_2 at 72 m sliding distance given in Figure 4.a. This sudden increase in the weight loss results from a large particle breaking off the material during wear [18, 37]. The wear rate results support these results, as well. What is expected in the wear test results is an increase in sliding distance and decrease in weight loss. As expected, the lowest weight loss was recorded at 0.6 ms^{-1} sliding speed. However, contrary to expectations, the highest weight loss was observed at 0.4 ms^{-1} sliding speed. The decrease in the weight loss at 0.6 ms^{-1} sliding speed results from the protective effect of the oxide layer forming on the surface. As the sliding speed increases, the increasing temperature resulting from friction leads to the formation of a more effective (protective) oxide layer on the surface. Due to the lubricating feature of the emerging oxide layer, the weight loss decreases [17, 38]. On the other hand, the highest weight loss obtained at 0.4 ms^{-1} sliding speed can be explained with the breaking of the oxide layer forming on the surface. Similar results were reported in a previously conducted study [39]. Furthermore, the friction coefficient results given in Figure 5 support these results. Friction coefficients of the AMC materials produced with the addition of different amounts of ZrO_2 are given in Figure 5.

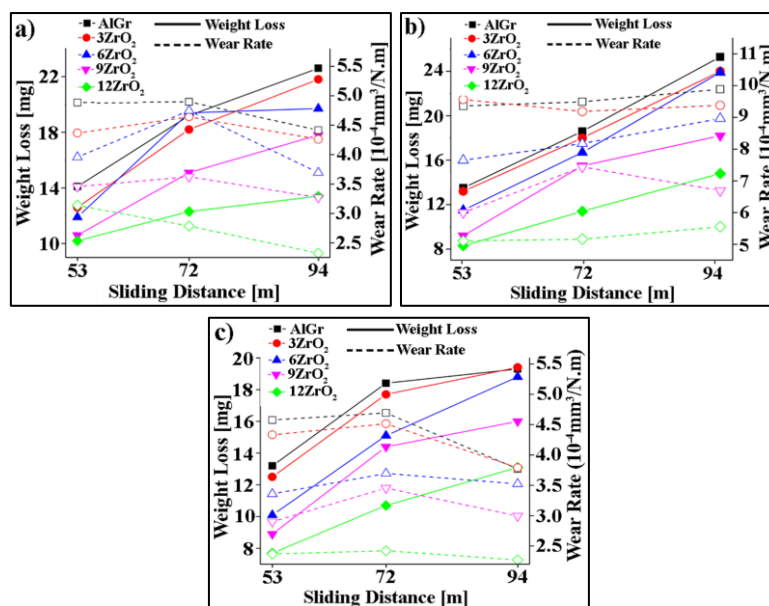


Figure 4. Weight losses and wear rates of composite materials with different amounts of ZrO_2 reinforced; 0.2 ms^{-1} (a), 0.4 ms^{-1} (b), and 0.6 ms^{-1} (c).

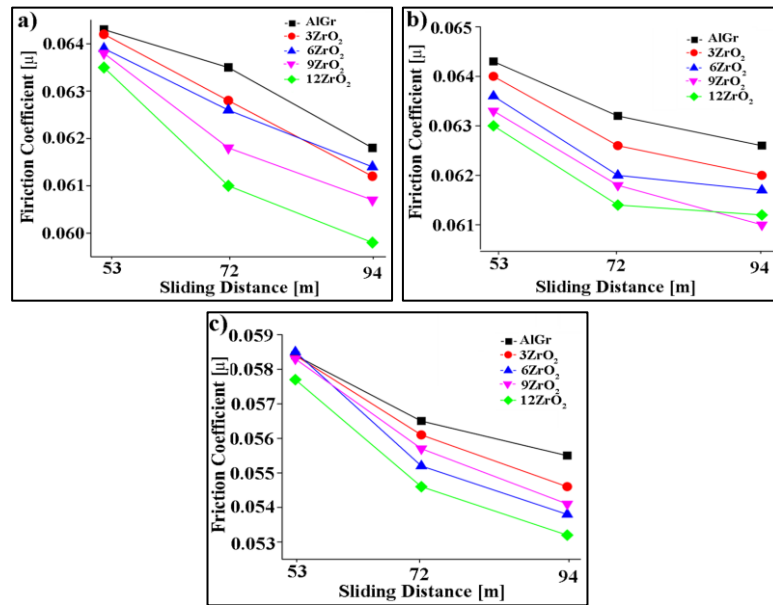


Figure 5. Friction coefficients of composite materials with different amounts of ZrO₂ reinforced; 0.2 ms⁻¹ (a), 0.4 ms⁻¹ (b), and 0.6 ms⁻¹ (c).

When the friction coefficients of the AMC materials containing different amounts of ZrO₂ at different sliding speeds as given in Figure 5 are examined, it is seen that the friction coefficient decreases as the amount of reinforcement increases. This decrease in the friction coefficient results from the decrease in disc/sample contact surface as the amount of reinforcement into the matrix increases. On the other hand, it is expected that the friction coefficient of the material with high hardness value is low [18]. The decrease in the friction coefficient is compatible with the hardness results given in Figure 3. Also, it is seen that the friction coefficient decreases along with increasing sliding distances at all sliding speeds. Accordingly, the friction coefficient decreases due to the protective oxide layer forming on the surface and also the solid lubricating effect of the graphite within the matrix [32, 38]. On the other hand, it is expected that the friction coefficient decreases as the sliding speed increases. While these results are obtained in short sliding distances (53 m and 72 m), it is not in question in longer sliding distances (94 m). Especially after 72 m sliding distance at 0.4 ms⁻¹ sliding speed, when the friction coefficients are compared to the other sliding speeds, they are found to be high. This increase in the friction coefficients is attributed to the increase in the sample surface roughness. The increase in the weight loss in the weight loss results given Figure 4.b is a clear indicator of this situation. Also, the worn surface SEM images given in Figure 6.b support this finding. The worn surface SEM images of the AMC materials containing 12% ZrO₂ at different sliding speeds are given in Figure 6.

When the worn surface SEM images of the AMC materials containing 12% ZrO₂ at different sliding speeds given in Figure 6 are examined, the spalls occurring on the worn surface at all sliding speeds can be clearly observed.

Deformation marks can be clearly observed in the worn surface obtained at 0.6 ms⁻¹ sliding speed (Figure 6.c). However, when the worn surfaces with 0.6 ms⁻¹ sliding speed are compared with the worn surfaces obtained at other sliding speeds, it is seen that traces of deformation disappear, and a more planar surface is formed. It is thought that the heat released by friction with increased sliding speed and the protective effect of the hard oxide layer formed on the surface are caused by the increase of wear resistance. It is stated that similar results were obtained in a previous study [37]. Also, it is understood that the fractures in sheet form observed on the worn surface obtained at 0.4 ms⁻¹ sliding speed (Figure 6.b) are more apparent and abundant when compared to the worn surfaces obtained at the other speeds (0.2 ms⁻¹ and 0.6 ms⁻¹). The weight loss and friction coefficient results obtained in the study support this situation, as well. The worn surface mapping images of the AMC materials containing 12% ZrO₂ at different sliding speeds are given in Figure 7.

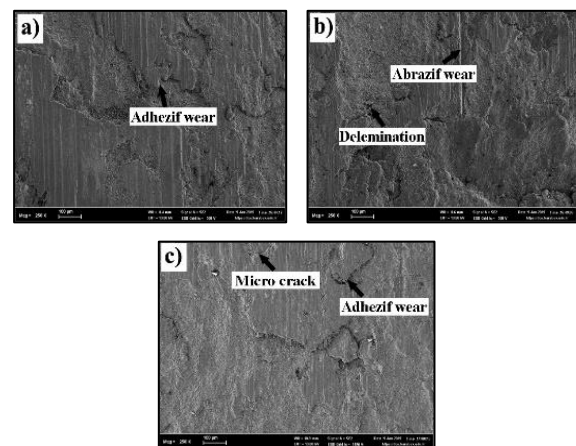


Figure 6. SEM images of worn surfaces on different sliding speed of composite materials with added 12% ZrO₂ a) 0.2 ms⁻¹, b) 0.4 ms⁻¹, c) 0.6ms⁻¹

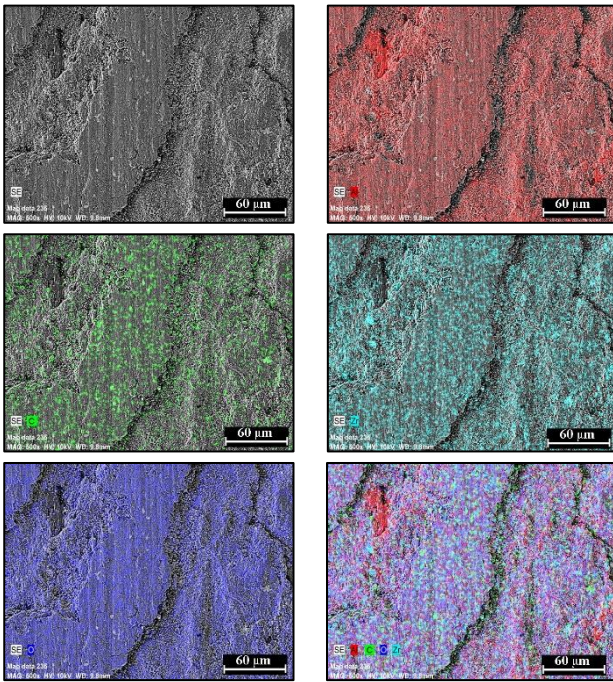


Figure 7. Worn surface mapping images of different sliding speed of composite materials with added 12% ZrO₂

When the mapping images of the AMC materials containing 12% ZrO₂ at 0.6 ms⁻¹ sliding speed given in Figure 6 are examined, the oxide layer formed on the surface is clearly understood. In the SEM images given in Figure 1, it is understood that the reinforcing material (ZrO₂) cluster especially on the grain boundaries is disperse on the worn surface. It is believed that ZrO₂, which is clustered at grain boundaries, is caused by re-burial on the sample surface without leaving the tribological system during wear. Due to weak particle binding, surface contamination and oxidation, micro cracks form on the sample surface as a result of a series of successive events. The formation of scaly spills, deep grooves, pits with the progression of the formed micro cracks causes delamination on the worn surface. The worn surface SEM images given in Figure 6 clearly show the delamination areas. The worn surface SEM images given in Figure 6 clearly show the delamination areas. In addition, it is observed that there are regional adhesive and abrasive wear mechanisms on the wear surfaces.

4. Conclusions

The results reached in the study where the wear behaviours of the AMC materials containing different amounts of ZrO₂ added into AlGr matrix at different sliding speeds were examined are as follows:

- ZrO₂ particles added into the matrix at different amounts get lumpy in the structure and are located on the grain boundaries, in particular.
- In XRD analysis results, Al₄C₃ phase, which was expected to form in the matrix (AlGr) material, could

not be encountered. On the other hand, the expected Al₄C₃ phase and Al₃Zr phase were observed in XRD results of the AMC material containing 12% ZrO₂.

- According to the hardness results, hardness of the AMC material increased as the amount of added reinforcement material increased, and the highest hardness value was obtained in the AMC material containing 12% ZrO₂.
- According to the density results, density of the AMC materials increased as the amount of added reinforcement material increased, and the highest density was obtained in the AMC material containing 12% ZrO₂.
- In the wear test results, lowest weight loss and wear rate were obtained at 0.6 ms⁻¹.
- According to the results related to friction coefficient, the lowest friction coefficient was obtained at 0.6 ms⁻¹ sliding speed.

Declaration

The author(s) declared no potential conflicts of interest with respect to the research, authorship, and/or publication of this article. The author(s) also declared that this article is original, was prepared in accordance with international publication and research ethics, and ethical committee permission or any special permission is not required.

References

1. Das, S., Das, S., and Das, K., *Abrasive wear of zircon sand and alumina reinforced Al-4.5 wt%Cu alloy matrix composites-A comparative study*. Composites Science and Technology, 2007. **67**(3-4): p. 746-751.
2. Idusuyi, N., and Olayinka, J. I., *Dry sliding wear characteristics of aluminium metal matrix composites: a brief overview*. Journal of Materials Research and Technology. 2019, **8**(3): p. 3338-3346.
3. Hemanth, J., *Tribological behavior of cryogenically treated B₄Cp/Al-12%Si composites*. Wear, 2005. **258**: p. 1732-1744.
4. Özyürek, D., Tekeli, S., *An investigation on wear resistance of SiCp-reinforced aluminium composites produced by mechanical alloying method*. Science and Engineering of Composite Materials, 2010. **17**(1): p. 31-38.
5. Çam, S., Demir, V., and Özyürek, D., *Wear behaviour of A356/TiAl₃ in situ composites produced by mechanical alloying*. Metals, 2016. **6**: p. 34-42.
6. Parvin, N., Assadifard, R., Safarzadeh, P., Sheibani, S., and Marashi, P., *Preparation and mechanical properties of SiC-reinforced Al6061 composite by mechanical alloying*. Materials Science and Engineering A, 2008. **492**: p. 134-140.
7. Sozhamannan, G.G., Yusuf, M.M., Aravind, G., Kumaresan, G., and Velmurugan, K., Venkatachalapathy, V.S.K., *Effect of applied load on the wear performance of 6061 Al/ nano TiCp/ Gr hybrid composites*. Materials Today: Proceedings, 2018. **5**: p. 6489-6496.
8. Şimşek, D., Şimşek, İ., Özyürek, D., *Production and Characterization of Al-SiC Composites by Mechanical Milling*. BEÜ Fen Bilimleri Dergisi, 2019. **8** (1): p. 227-233.

9. Zi-yang, X., Guo-qin, C., Gao-hui, W., Wen-shu, Y., and Yan-mei, L., *Effect of volume fraction on microstructure and mechanical properties of Si3N4/Al composites*. Transaction of Nonferrous Metals Society of China, 2011. **21**: p. 285-289.
10. Ahamed, H., and Senthilkumar, V., *Role of nano-size reinforcement and milling on the synthesis of nano-crystalline aluminium alloy composites by mechanical alloying*. Journal of Alloys and Compounds, 2010. **505**: p. 772-782.
11. Zhu, H., Jar, C., Song, J., Zhao, J., Li, J., and Xie, Z., *High temperature dry sliding friction and wear behavior of aluminum matrix composites (Al₃Zr₃Al₂O₃)/Al*. Tribology International, 2012. **48**: p. 78-86.
12. Özyürek, D., Tuncay, T., Evlen, H., and Çiftci, I., *Synthesis, characterization and dry sliding wear behavior of in-situ formed TiAl₃ precipitate reinforced A356 alloy produced by mechanical alloying method*. Materials Research, 2015. **18**(4): p. 813-820.
13. Torralba, J.M., da-Costa, C.E., and Velasco, F., *P/M aluminum matrix composites: an overview*. Journal of Materials Processing Technology, 2003. **133**: p. 203-206.
14. Durai, T.G., Das, K., Das, S., *Corrosion behavior of Al-Zn/Al₂O₃ and Al-Zn-X/Al₂O₃ (X=Cu, Mn) composites synthesized by mechanical-thermal treatment*. Journal of Alloys and Compounds, 2008. **462**: p. 410-415.
15. Aksoz, S., Bican, O., Calin, R., and Bostan, B., *Effect of T7 heat treatment on the dry sliding friction and wear properties of the SiC-reinforced AA 2014 aluminium matrix composites produced by vacuum infiltration*. Proceedings of the Institution of Mechanical Engineers, Part J: Journal of Engineering Tribology, 2013. **228**(3): p. 312-319
16. Özyürek, D., and Tekeli, S., *An investigation on wear resistance of SiCp-reinforced aluminum composites produced by mechanical alloying*. Science and Engineering of Composite Materials, 2010. **17**(1): p. 31-38.
17. Şimşek, İ., Şimşek, D. Özyürek, D., *Investigation of the Effect of Ni Amount on the Wear Performance of A356 Cast Aluminum Alloys*. Metallurgist (2020). <https://doi.org/10.1007/s11015-020-00917-w>
18. Özyürek, D., Tekeli, S., Güral, A., Meyveci, A., and Gürü, M., *Effect of Al₂O₃ amount on microstructure and wear properties of Al-Al₂O₃ metal matrix composites prepared using mechanical alloying method*. Powder Metallurgy and Metal Ceramics, 2010. **49**(5-6): p. 50-57.
19. Özyürek, D., and Tekeli, S., *Wear properties of titanium and Ti6Al4V titanium alloy by mechanical milling*. High Temperature Materials and Processes, 2011. **30**(1-2): p. 175-180.
20. Aydın, D.Y., Gürü, M., Ipek, D., and Özyürek, D., *Synthesis and characterization of zinc fluoroborate from zinc fluoride and boron by mechanochemical reaction*. Arabian Journal for Science and Engineering, 2017. **42**: p. 4409-4416.
21. Aztekin, H., Özyürek, D., and Çetinkaya, K., *Production of hypo-eutectic Al-Si alloy based metal matrix composite with thixomoulding processing*. High Temperature Materials and Processes, 2010. **29**(3): p. 169-178.
22. Özyürek, D., *The effect of semi-solid processing parameters on microstructure in Al-7wt.%Si alloy*. Scientific Research and Essays, 2011. **6**(29): p. 6222-6226.
23. Özyürek, D., Yıldırım, M., and Çiftçi, İ., *The tribological properties of A356-SiCp metalmatrix composites fabricated by thixomoulding technique*. Science and Engineering of Composite Materials, 2012. **19**(4): p. 351-356.
24. Prabhu, B., Suryanarayana, C., An, L., and Vaidyanathan, R., *Synthesis and characterization of high volume fraction Al-Al₂O₃ nanocomposite powders by high-energy milling*. Materials Science and Engineering A, 2006. **425**: p. 192-200.
25. Wang, Y.Q., and Song, J.I., *Temperature effects on the dry sliding wear of Al₂O₃/SiCp/Al MMCs with different fiber orientations and hybrid ratios*. Wear, 2011. **270**: p. 499-505.
26. Zhu, H.G., Ai, Y.L., Min, J., Wu, Q., and Wang, H.Z., *Dry sliding wear behavior of Al-based composites fabricated by exothermic dispersion reaction in an Al-ZrO₂-C system*. Wear, 2010. **268**: p. 1465-1471.
27. Baghchesara, M.A., Abdizadeh, H., Baharvandi, H.R., *Microstructure and mechanical properties of aluminum alloy matrix composite reinforced with ZrO₂ particles*. Asian Journal of Chemistry, 2010. **22**(5): p. 3824-3834.
28. Ramachandra, M., Abhishek, A., Siddeshwar, P., and Bharathi, V., *Hardness and wear resistance of ZrO₂ nano particle reinforced Al nanocomposites produced by powder metallurgy*. Procedia Materials Science, 2015. **10**: p. 212-219.
29. Şimşek, İ., Yıldırım, M., Özyürek, D. and Şimşek, D. *Basıncısız infiltrasyon yöntemiyle üretilen SiO₂ takviyeli alüminyum kompozitlerin aşınma davranışlarının incelenmesi*. Politeknik Dergisi, 2019, **22**(1): p. 81-85.
30. Şimşek, İ., Şimşek, D. and Özyürek, D. *Investigation of the Effect of Ni Amount on the Wear Performance of A356 Cast Aluminum Alloys*. Metallurgist, 2020, **63**(9-10): p. 993-1001.
31. General Directorate of Highways, "Vehicle Stopping and Transfer Times", Turkey <http://www.kgm.gov.tr/Sayfalar/KGM/SiteTr/Trafik/DurmaIntikal.aspx>. (last access date:17.09.2019)
32. Simsek, I., *The effect of B₄C amount on wear behaviors of Al-Graphite/B₄C hybrid composites produced by mechanical alloying*. Journal of Boron, 2019. **4**(2): p. 100-106.
33. Chu, H.S., Liu, K.S., and Yeh, J.W., *Damping behavior of in situ Al-(graphite, Al₄C₃) composites produced by reciprocating extrusion*. Journal of Materials Research, 2001. **16**(5): p. 1372-1380.
34. Sekar, K., Jayachandra, G., and Aravindan, S., *Mechanical and welding properties of A6082-SiC-ZrO₂ hybrid composite fabricated by stir and squeeze casting*. Materials Today: Proceedings, 2018. **5**: p. 20268-20277.
35. Bostan, B., Ozdemir, A.T., and Kalkanli, A., *Microstructure characteristics in Al-C system after mechanical alloying and high temperature treatment*. Powder Metallurgy, 2004. **47**(1): p. 37-42.
36. Kumar, K.R., Pridhar, T., and Sree, V.S., *Mechanical properties and characterization of zirconium oxide (ZrO₂) and coconut shell ash(CSA) reinforced aluminium (Al 6082) matrix hybrid composite*. Journal of Alloys and Compounds, 2018. **765**: p. 171-179
37. Rao, R. N. and Das, S. *Effect of SiC content and sliding speed on the wear behaviour of aluminium matrix composites*. Materials & Design, 2011, **32**(2): p. 1066-1071.
38. Özyürek, D., Tunçay, T., and Kaya, H., *The effects of T5 and T6 heat treatments on wear behaviour of AA6063 alloy*. High Temperature Materials and Processes, 2014. **33**(3): p. 231-237.
39. Özyürek, D, Ciftci, I., and Tuncay, T., *The effect of aging and sliding speed on wear behaviour of Cu-Cr-Zr alloy*. Materials Testing, 2013. **55**(6): p. 468-471.